Liquid Crystals
Publication details, including instructions for authors and subscription information:
http://www.informaworld.com/smpp/title~content=t713926090

An experimental investigation of discrete changes in pitch in a thin, planar chiral nematic device

H. G. Yoon[a]; N. W. Roberts[a]; H. F. Gleeson[a]
[a] School of Physics and Astronomy, The University of Manchester, Manchester M13 9PL, UK

To cite this Article Yoon, H. G. , Roberts, N. W. and Gleeson, H. F.(2006) 'An experimental investigation of discrete changes in pitch in a thin, planar chiral nematic device', Liquid Crystals, 33: 4, 503 — 510
To link to this Article: DOI: 10.1080/02678290600633501
URL: http://dx.doi.org/10.1080/02678290600633501

Liquid Crystals, Vol. 33, No. 4, April 2006, 503–510

An experimental investigation of discrete changes in pitch in a thin, planar chiral nematic device

H.G. YOON, N.W. ROBERTS and H.F. GLEESON*
School of Physics and Astronomy, The University of Manchester, Manchester M13 9PL, UK

(*Received 9 January 2006; accepted 1 February 2006*)

The phenomenon whereby sudden changes in helicoidal pitch occur in thin chiral nematic devices with strong surface anchoring has been studied experimentally. This has been done with the aim of examining the underlying process in the context of existing theory. Thin devices (~2.5 μm thick) containing two commercially available chiral nematic liquid crystals were employed in the study. The samples were chosen for their dependence of pitch on temperature; one exhibits a very slow increase in pitch with increasing temperature (95.6% of the Merck material BL131 in BL130), while the second shows the more common rapid reduction in pitch with increasing temperature (the Merck mixture TM1001). High resolution reflection spectra were obtained for the devices and a numerical fitting algorithm, based on the Berreman 4×4 matrix technique, provided accurate information on changes in the pitch, refractive indices, device thickness and changes in the surface director across the pitch jump region. We demonstrate that changes in refractive index and device thickness are negligible in analysis of the reflection spectra across the pitch jumps. We further show that the pitch changes discontinuously at the pitch jump, with no variation in its value as the process occurs. We find evidence that the surface directors also change by less than 10° during this process in a manner analogous to coiling or uncoiling a constrained spring. This mechanism differs somewhat from others proposed in the literature.

1. Introduction

The selective reflection of light from a chiral nematic (N*) liquid crystal is one of the best known optical phenomena in liquid crystals. The marked temperature dependence of the selective reflection wavelength is commonly employed in devices such as liquid crystal thermometers. In planar devices in which the director is anchored on the top and bottom surfaces of the device, the helix is generally considered to adopt a whole number of half-pitches across the device thickness [1]. As the temperature is changed, so-called pitch jumps occur which are easily observable as changes in the selective reflection wavelength. There have been several reports of thermal hysteresis in the pitch jumps [2–4], as well as theoretical treatments that relate the hysteresis to parameters including surface anchoring and cell thickness [5–8].

Zink and Belyakov [5] explained the discrete changes in pitch of a chiral nematic liquid crystal through a minimization of the free energy that includes terms in the twist energy and the surface anchoring energy. They argued that a reduction in the thickness of a chiral nematic liquid crystal device increases the effect of the surface anchoring energy with respect to the twist energy. Both factors are temperature dependent, but the pitch and therefore the twist energy usually changes more rapidly with temperature. In thin devices, where the surface anchoring energy is the dominant term, the change in twist energy associated with a pitch change must be sufficient to overcome the surface anchoring barrier before a pitch jump can occur. Zink and Belyakov further used the pitch jump process to explain the phenomena of thermal hysteresis [6] and helix inversion [9]. They analysed the spectra obtained experimentally by superposition of two different pitch states, where a key parameter was the anglular deviation of the surface director.

The majority of published experimental studies of selective reflection from chiral nematic films rely on the measurement of the selective reflection wavelength, λ_o, rather than direct measurement of the pitch, p. Although λ_o is closely related to p, it is only actually proportional to it through the well known equation $\lambda_o = \bar{n}p$, if the dispersion of the average refractive index, $\bar{n}$, is taken into account [10]. The inaccuracy introduced by this approximation becomes significant when very small changes in pitch are to be measured. In this paper

---

*Corresponding author. Email: helen.gleeson@manchester.ac.uk

Liquid Crystals
ISSN 0267-8292 print/ISSN 1366-5855 online © 2006 Taylor & Francis
http://www.tandf.co.uk/journals
DOI: 10.1080/02678290600633501

we report high resolution spectral measurements of the selective reflection from chiral nematic liquid crystal devices at normal incidence. We use an accurate fitting technique [10, 11] to deduce the pitch, surface director orientation, device thickness, refractive indices and dispersion in the refractive indices, thereby allowing us to examine the pitch jump process in detail.

2. Theoretical background

Zink and Belyakov have theoretically considered the phenomenon of pitch jumps in chiral nematic liquid crystals in detail [5, 6]. They described how at temperatures close to the pitch jump, there is an opposite reorientation of the director at both surfaces due to the competition between the twist energy of the helix and the restoring forces of the surface anchoring potentials. This asymmetry is a fundamental assumption in their theory describing pitch jump. They showed that in the region of a pitch jump, the free energy of a planar chiral nematic liquid crystal sample might be expressed as:

$$F = 2W_{\mathrm{s}}(\varphi) + K_{22}[2\pi/p_{N+\Delta N} - 2\pi/p(T)]^2 p_{N+\Delta N}(N+\Delta N)/4 \qquad (1)$$

where K_{22} is the twist elastic constant, N is the integer number of half-turns in the cell before the pitch jump, ΔN is the non-integer number of half pitches in the cell near to the pitch jump process, $p(T)$ is the equilibrium pitch, φ is the direction of the surface director with respect to the minimum (usually the rubbing direction) and $W_{\mathrm{s}}(\varphi)$ is the surface anchoring energy. As such, ΔN can be related to the changing angle between the directors at the top and bottom surfaces of the device. Therefore, the free energy expression essentially comprises one term that describes the energy cost of moving away from the minimum of the surface anchoring potential and another that expresses the twist energy in terms of the equilibrium pitch of the system and the actual pitch described by an integer number of half-turns plus a variable non-integer number of half turns due to the changing director orientation.

From equation (1), Zink and Belyakov went on to show the deviation angle of the surface director, φ_{j}, can be expressed as

$$\begin{aligned}\varphi_{\mathrm{j}} &= \pi/4 - d(\partial W_{\mathrm{s}}/\partial\varphi)/K_{22} \\ &= \pi/4 - (d/p)(\partial W_{\mathrm{s}}/\partial\varphi)/(K_{22}/p)\end{aligned} \qquad (2)$$

When a Rapini potential is used to describe the surface energy, equation (2) became

$$\sin 2\varphi_{\mathrm{j}} - (2K_{22}/Wd)\left(\varphi_{\mathrm{j}} - \pi/4\right) = 0. \qquad (3)$$

Here, $4K_{22}/pW$ is the ratio of the bulk energy of twisting per turn of the helix to the surface anchoring energy.

According to the theory, the surface director will have a maximum deviation angle, φ_{c}, where the twist energy just overcomes the surface anchoring energy, expressed as:

$$\varphi_{\mathrm{c}} = \pi\left[\frac{2d}{p_d(T_{\mathrm{c}})} - N\right]. \qquad (4)$$

Here, d is the device thickness, N is number of half turns and $p_d(T_{\mathrm{c}})$ is the pitch before the pitch jump takes place. At the critical point of a pitch jump, the deviation angle is equal to the critical angle, $\varphi_{\mathrm{j}}=\varphi_{\mathrm{c}}$. In the case of strong surface anchoring, rotation of the director at the surface (due to changes in the twist energy as temperature is changed) is predicted to be hindered. Moreover, in a device where the anchoring energy dominates over the twist elastic energy, φ_{c} will be large. Conversely, in thick devices where the twist energy term dominates, the result is reversed. The anchoring energy term also affects the thermal hysteresis so that if the free energy of the system is dominated by the twist, as may happen in a weak anchoring potential, then the director rotation at the surface is a completely reversible process and no hysteresis is observed. Alternatively, if the anchoring term dominates, hysteresis may well be observed. Measurement of the critical angle is clearly implicated in understanding the pitch jump process.

3. Experimental

3.1. *Materials and devices*

The two liquid crystal mixtures investigated in this study, BL131/130 and TM1001 are both produced by Merck Ltd, Lutterworth, UK, and their phase sequences are given in figure 1. The BL131/130 mixture has an extremely broad chiral nematic phase with no close underlying smectic A (SmA) phase. It has been shown previously that the pitch increases slightly with increasing temperature [12]. The mixture TM1001 exhibits a room temperature SmA phase and the helicoidal pitch consequently undergoes critical divergence at the SmA–N* transition.

Devices were constructed in-house from non-conducting glass, ensuring that the conductive layer need

BL131/130 95.6% : N* $\overset{104\,^{\circ}\mathrm{C}}{\rightleftarrows}$ I

TM1001 : Sm-A $\overset{27\,^{\circ}\mathrm{C}}{\rightleftarrows}$ N* $\overset{44\,^{\circ}\mathrm{C}}{\rightleftarrows}$ I

Figure 1. Phase transition temperatures for the materials used in this investigation. All temperatures are as provided by Merck Ltd and confirmed by polarizing microscopy.

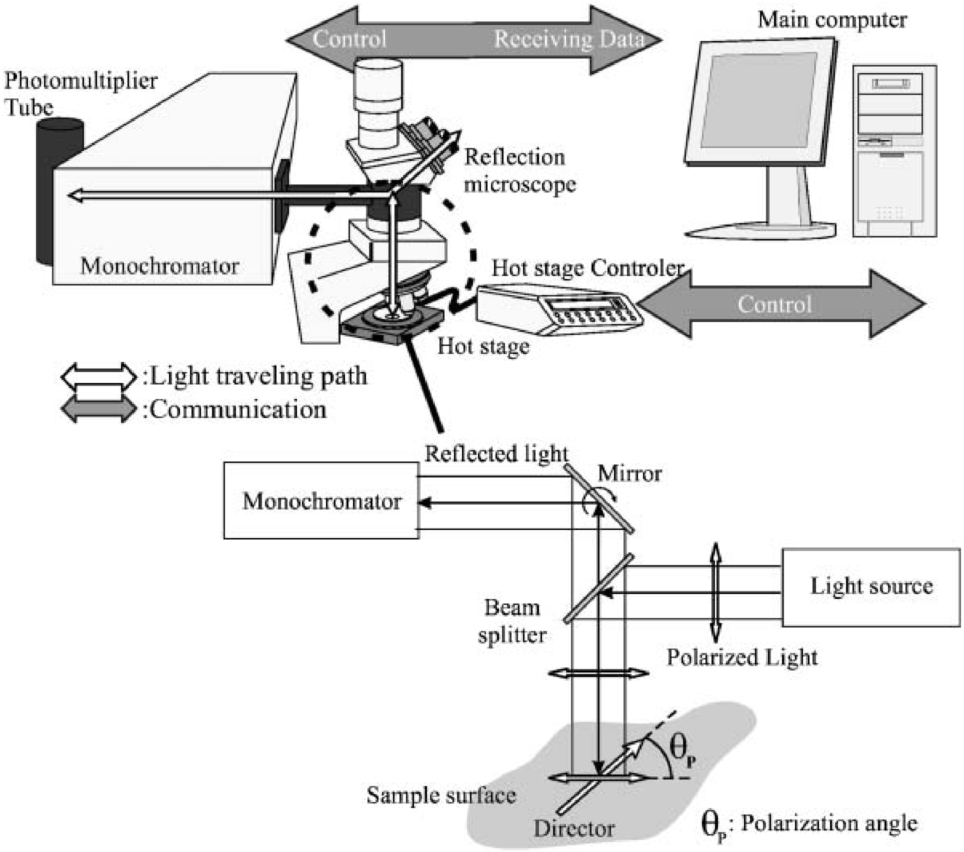

Figure 2. Schematic drawing of the equipment used to measure selective reflection spectra. Linearly polarized light is incident on the sample surface and the reflected light is guided to the monochromator.

not be taken into account when fitting the experimental data to theory. The inner surfaces of the glass were coated with rubbed polyvinyl alcohol alignment layers to promote excellent planar alignment of the sample. The cell thickness used for the experiments on the BL131/130 95% and the TM1001 mixtures were 2.51 ± 0.02 µm and 2.64 ± 0.02 µm respectively (measured using interferometry).

3.2. *Apparatus*

The optical properties of the chiral nematic devices were studied in a reflection geometry, using a specially designed computer-controlled apparatus that allows the peak selective reflection wavelength to be measured with an accuracy of ±0.2 nm at temperature intervals of 0.1°C [11]. The apparatus is shown schematically in figure 2 and makes use of a reflective polarizing microscope linked optically to a monochromater to analyse the reflected light. The microscope contains a high quality Glan–Taylor polarizer to define the input polarization direction. A low numerical aperture objective allows the chiral nematic liquid crystal to be studied at effectively normal incidence [10]. The sample area analysed is approximately 2 mm in diameter. Reflection spectra are recorded between 400 and 700 nm with an accuracy of ±0.1 nm. The temperature gradient across the field of view was measured to be <0.2°C by determining the range over which the nematic to istotropic phase transition took place in the pure material pentylcyanobiphenyl (5CB).

3.3. *Spectral analysis*

As already mentioned, the peak wavelength of a selective reflection spectrum at normal incidence is generally described by the simple equation $\lambda_o=\bar{n}p$ while the bandwidth is given by $\Delta\lambda=\Delta n p$, where $\Delta\lambda$ is the width of the reflection spectrum and Δn is the birefringence. However, these equations assume that the refractive index is a constant with respect to wavelength and accurate modelling of reflection spectra or fitting to data must allow for the fact that refractive indices are subject to dispersion. This can be done adequately by the use of Sellmeier's equation [14, 15], $n=\left[1+A\,\lambda^2\left(\lambda^2-B^2\right)^{-1}\right]^{\frac{1}{2}}$, where the coefficients A and

B are material and temperature dependent. Our previous work [11] has shown that, in spite of possible degeneracy in the theoretical fits to the data (a consequence of the fact that a product of the refractive indices and cell thickness describes some of the optics of the system), we can accurately fit theoretically predicted spectra to experimental data using a Simplex minimization method. Using this technique, we obtain accurate values, for the refractive indices n_o and n_e and their wavelength dependence (± 0.001), the sample thickness d ($\pm 0.01\,\mu$m), the pitch (± 0.1 nm) and the relative orientation of the surface director with respect to the polarization direction of the incident light, the polarization angle, θ_p in figure 2 ($\pm 2°$).

Generally, the device thickness defines the properties of the interference peaks while the pitch and birefringence define the position and width of the main selective reflection peak. The polarization direction of the incident light has a significant effect on the profile of the selective reflection peak [10]. Furthermore, the combined measurement of the pitch, thickness and the polarization angle provides an explicit method to detect a change in the deviation angle, as defined in the theory section and equation (3). It would be expected that if the deviation angle changes as a function of temperature, then measurements of the pitch and polarization angle should also show variation. Therefore, this experimental approach is ideal for the study of the pitch jump process where small changes in the pitch and the orientation of the surface director are sought. The fact that all the relevant parameters are deduced ensures that small changes in refractive index with temperature, or indeed device thickness, can be accounted for in considering any change in shape of the reflection spectra during the pitch jump process.

4. Results

4.1. *Analysis of the measured reflection spectra*

Reflection spectra were measured at 0.1°C intervals for both samples on heating and on cooling across the pitch jump regions. Pitch jumps of +26.6 nm in the BL130/131 (at 63.9°C) mixture and −21.6 nm in the TM1001 (at 32.4°C) mixture were observed within the devices, together with thermal hysteresis effects, confirming that the devices were in the strong anchoring regime. In the experimental arrangement, light was collected from a 2 mm diameter area on the sample. There are two experimental situations to consider. Well away from the pitch jump regime, the sample area contained a single pitch domain and the reflection spectrum is formed by a single selective reflection peak, see figure 3. However, at temperatures in the pitch jump regime, the sample area contained two regions of differing pitch and the reflection spectrum is therefore a superposition of two spectra. Each situation is considered separately below as slightly different analysis techniques were employed to fit the experimental data.

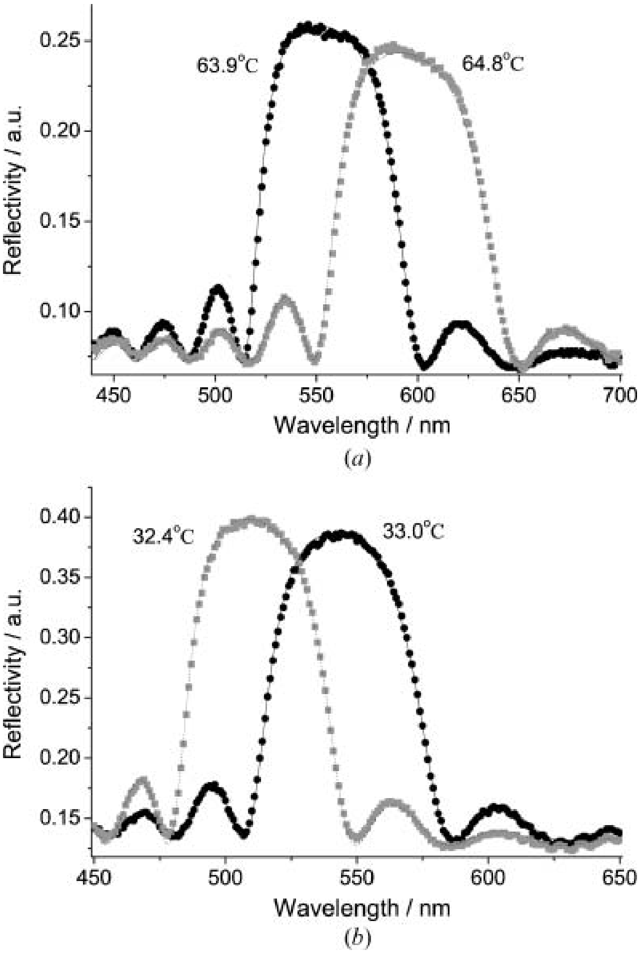

Figure 3. A comparison of experimental data (circles) and fitted spectra (solid lines) for (*a*) the BL131/130 mixture and (*b*) the TM1001 mixture before and after the pitch jump has occurred. Parameter values for these spectra are given in table 1.

4.2. *Analysis of single pitch sample areas*

Figure 3 shows two typical spectra from each material obtained from the low and high temperature regions either side of the pitch jump. The experimental data and the best fits to the optical theory are both shown and table 1 details the minimized fitting parameters for each of the theoretical fits. As already mentioned, the fits determine the helicoidal pitch, the device thickness, the Sellmeier coefficients (and therefore n_o and n_e) and the angle made between the input polarization and the surface director (the polarization angle). In our

Table 1. Fitting results for the experimental data for the BL131/130 and TM1001 spectra shown in figure 3. Note that in determining the polarization angle, the absolute value is arbitrary (depending only on how the sample was placed in the apparatus), but relative changes in this parameter provide information on changes in the surface director orientation.

Mixture	Fitting Parameters		Pre-jump	Post-jump
BL131/130 mixture	Refractive index n_o	Sellmeier Coefficient *A*/nm	1.584 ± 0.001	1.584 ± 0.001
		Sellmeier Coefficient *B*/nm	139 ± 1	139 ± 1
	Refractive index n_e	Sellmeier Coefficient *A*/nm	1.186 ± 0.001	1.186 ± 0.001
		Sellmeier Coefficient *B*/nm	120 ± 1	120 ± 1
	Device thickness/µm		2.51 ± 0.01	2.51 ± 0.01
	Pitch/nm		353.9 ± 0.1	380.5 ± 0.1
	Polarization angle/degrees		51 ± 2	55 ± 2
TM1001	Refractive index n_o	Sellmeier Coefficient *A*/nm	1.526 ± 0.001	1.526 ± 0.001
		Sellmeier Coefficient *B*/nm	101 ± 1	101 ± 1
	Refractive index n_e	Sellmeier Coefficient *A*/nm	1.188 ± 0.001	1.188 ± 0.001
		Sellmeier Coefficient *B*/nm	109 ± 1	109 ± 1
	Device thickness/µm		2.64 ± 0.01	2.64 ± 0.01
	Pitch/nm		350.9 ± 0.1	329.3 ± 0.1
	Polarization angle/degrees		47 ± 2	45 ± 2

experimental arrangement, the absolute value of the polarization angle is arbitrary (depending on how the sample was placed in the apparatus). However, changes in this angle and the values of the pitch, provide a direct measure of the deviation angle defined by Zink and Belyakov and set out in the above theory section.

The data shown in table 1 and similar data at other temperatures near the pitch jump indicate that either side of the pitch jump only two parameters, the pitch and the polarization angle, show any variation.

4.3. *Analysis of areas containing two pitch regions*

At temperatures close to the pitch jump region, the reflection spectra are formed from a combination of the two pitch states observed across the microscope field of view. Thus, in order to analyse the combined spectra, two different pitch states must be superposed with an appropriate weight ratio. Examples of such spectra are shown in figure 4 where experimentally determined reflection spectra from the intermediate regime are shown together with calculated spectra, in this case from combinations of the data of figure 3.

A grid-search methodology was adopted, allowing variation in pitch and polarization angle of the two discrete spectra to determine the parameter set that provides the best fit to the data, determined by the minimum chi-squared value. The grid resolution was 1° in the polarization angle and 1 nm in the pitch. Figure 4 and table 2 show examples of the best fit spectra to the complex spectra.

Table 2 shows that the grid resolution chosen matches well with our uncertainty in the theoretical fits obtained from the Simplex minimization routine. Importantly, the parameters obtained from the best fits to the combined spectra indicate there is no continuous change in the pitch as part of the pitch jump process; rather this parameter takes single discrete values before and after the jump.

The variation in pitch and the relative change in polarization angle across the pitch jump are shown on heating and cooling in figures 5 and 6, respectively. The temperature regimes where the single domain and multiple domains occur are clear from the pitch data (figure 5). As the thermal gradient across the field of view is <0.2°C, it can be concluded that hysteresis occurs in both samples, though it is more pronounced in the BL130/131 sample. It can also be seen that the change in the surface director angle in both samples across the pitch jump is rather small (<10°).

5. Discussion

The data obtained from these measurements allow us to calculate the critical angle and *N* defined in equation (4) from the theory of Zink and Belyakov. The data show that in the BL131/130 mixture, *N* changes from 14 to 13 either side of the jump, while in TM1001, *N* changes from 15 to 16 across the pitch change. Our data provide no evidence of any variation in the helical pitch before and after the jump and we have already noted that there is no change in the cell thickness with temperature. This also implies that in these mixtures the deviation angle does not change as a function of temperature or approach a critical value in the pitch jump regime. It is nonetheless possible to apply equation (4), using the values of the pitch and thickness determined experimentally, to calculate the deviation angle (i.e. the angle between the top and bottom surface directors) that is implied for the mixtures. It is found that the deviation

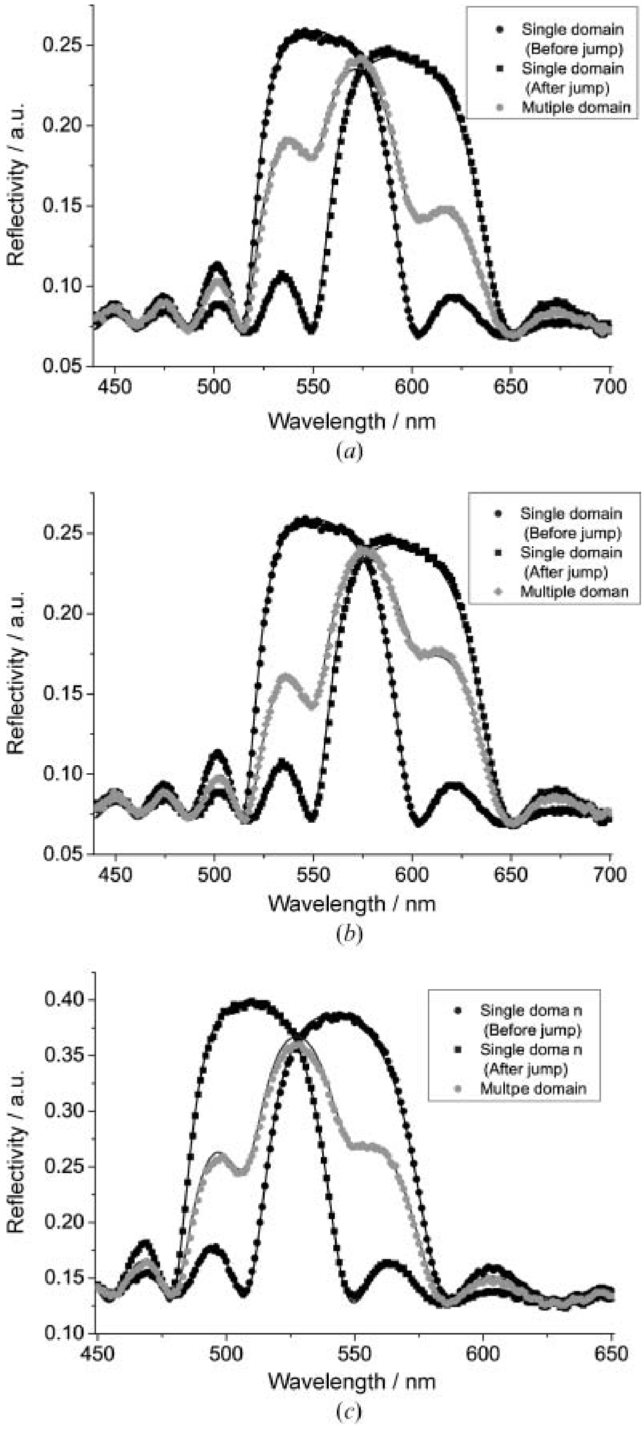

Figure 4. The best fit of two spectra in the pitch jump regime: (*a*) and (*b*) show data for the BL131/130 mixture at 64.3 and 64.4°C with weight ratios of 58:42 and 38:62 for the single pitch constituent spectra; (*c*) shows data for TM1001 at 32.7°C with a 56:44 ratio of constituent spectra.

angle in the BL131/130 mixture, is $33^\circ \pm 11^\circ$ on heating and $35^\circ \pm 11^\circ$ on cooling. Similarly the angle is $8^\circ \pm 10^\circ$ on heating and $6^\circ \pm 10^\circ$ on cooling for TM1001. Interestingly, these calculations indicate that while the director is effectively coincident with the rubbing direction for the TM1001 mixture, this is not the case for the BL131/130 mixture. Specifically, it seems that the directors at the top and bottom surfaces of the device have a minimum energy position that does not coincide with the rubbing direction. This observation is consistent with other measurements at different temperatures, and for other BL131/130 mixtures in different devices. Furthermore this situation has also been encountered in thin twisted nematic cells [15–17]. This phenomenon will be the subject of a future publication. Most importantly in our examination of the pitch jump process, our data show that the pitch jump is completely symmetric with respect to the surface director. This conclusion follows from the data of figure 5 and the knowledge that *d* remains constant.

Several other features can be seen in the data sets. Firstly, it is worth noting that the change in polarization angle is rather interesting. The variation in the polarization angle is much larger (around 10°) for the BL130/131 mixture than for the TM1001 material (<5°). In the BL130/131 mixture, there is strong evidence of an ‘intermediate’ distortion angle that occurs in the pitch jump regime. The data on heating and cooling show that one of the single pitch domains experiences a significant angular distortion, while the other does not. In fact, it seems that the hysteresis that occurs actually manifests where one of the ‘single pitch areas’ is rotated equally on both surfaces. On heating, it is the low temperature (old) pitch contribution that has a surface director angle of around 5°, and on cooling it is the high temperature (old) contribution that is distorted by around 5°. The implication is that where new pitch regions are being formed, the pitch and orientation angle are optimized, and it is the remnants of the old pitch state that are distorted. In the TM1001 mixture, the polarization angle before and after the pitch jump is the same—shown as 0° in figure 6 (*b*)—but during the pitch jump process, the angle again changes by around 5°. In this case the surface director distortion is slightly different; the surface director is distorted over a wider temperature range on cooling than on heating (approximately 0.7°C rather than 0.3°C). Again, it is the ‘old’ pitch state that is distorted while the new state has optimum pitch and orientation.

The fact that we observe a change in the polarization angle, but no change in pitch is worth dwelling on. Our technique is sensitive to both at the same time, so we can conclude from this that as the pitch jump takes place, the system is responding almost like a ‘coiled spring’. While the pitch does not actually change as part of the pitch jump process, the helicoidal structure is

Table 2. The best fit parameters from the grid-search. The parameter sets shown for each material have the same (minimum) chi-squared values. Pitch 1 and 2 and Angle 1 and 2 refer to the values for the two constituent spectra.

	Pitch/nm		Polarization angle/degree	
Sample	Pitch 1	Pitch 2	Angle 1	Angle 2
BL 131/130mixutre 64.3°C (58:42)	354.9	380.5	51	55
	354.9	380.5	52	54
	354.9	380.5	52	55
BL 131/130mixutre 64.4°C (38:62)	354.9	380.5	51	55
	354.9	380.5	52	54
	354.9	380.5	52	55
TM1001 32.7°C (56:44)	350.9	330.3	46	44

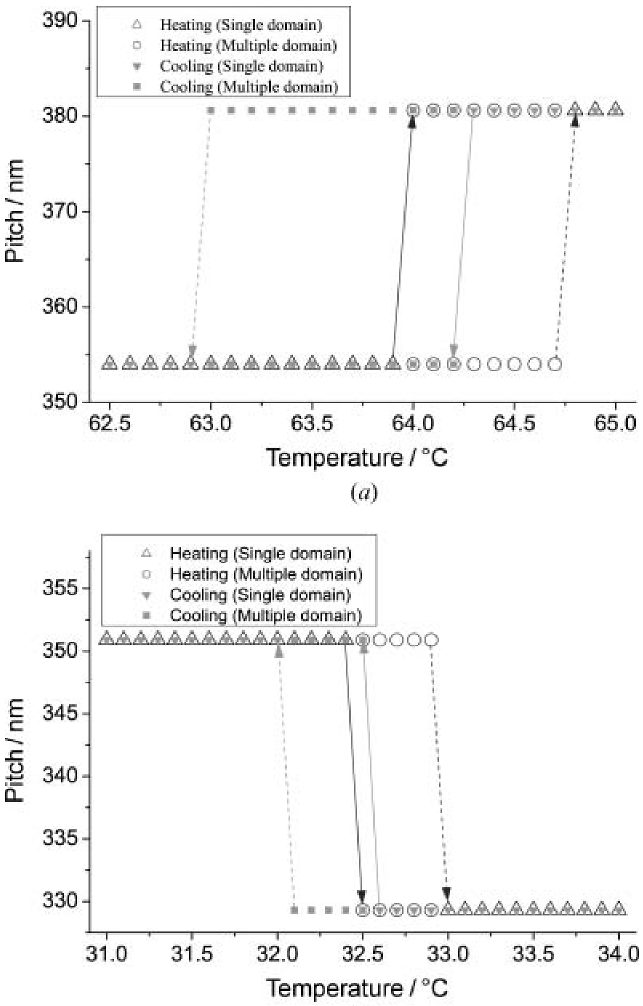

(*a*)

(*b*)

Figure 5. Experimental data showing the pitch variation as a function of temperature for (*a*) the BL131/130 mixture and (*b*) the TM1001 mixture on heating and on cooling.

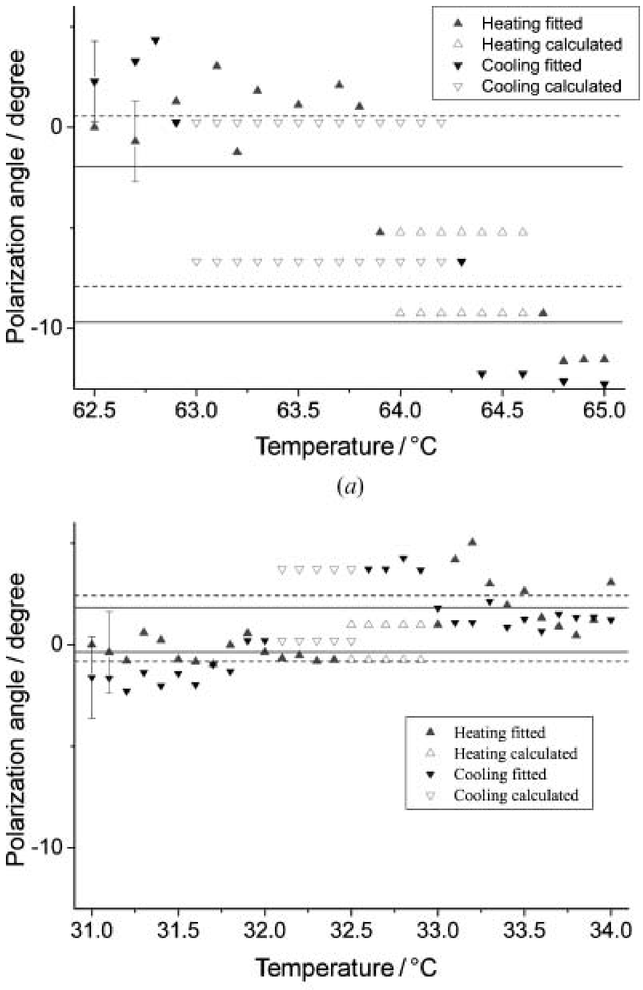

(*a*)

(*b*)

Figure 6. The polarization angle variation across the pitch jump. We changed the polarization angle to an absolute value for comparison with the deviation angle. (*a*) Data for the BL131/130 mixture, (*b*) data for TM1001. The solid horizontal line is a mean polarization angle during heating and the dashed line is a mean polarization angle during cooling.

rotated within the device in a manner consistent with a stressed helix. This is quite a different type of mechanism from that proposed by Belyakov and Zink.

6. Conclusion

The pitch jump process has been investigated in thin planar cholesteric devices containing two different chiral nematic materials. Experimentally, we observed both pitch jumps and thermal hysteresis in the samples, as would be expected for thin samples with strong surface anchoring. Excellent fits of the theory were obtained to the experimental data, allowing the surface director angle and the pitch to be accurately determined throughout the pitch jump process. Our data indicate that there is no continuous change in pitch associated with the pitch jump process; this is a truly discontinuous process. However, during the pitch jump process, the surface directors change in a manner consistent with coiling or uncoiling a spring. This is a surprising result, indicating that in our systems, the pitch value is extremely stable within the device.

References

[1] P.G. de Gennes, J. Prost. *The Physics of Liquid Crystals*. Oxford University Press, London (1993).

[2] G.D. Dixon, L.C. Scala. *Mol. Cryst. liq. Cryst.*, **10**, 317 (1970).

[3] J.V. Gandhi, X.-D. Mi, D.-K. Yang. *Phys. Rev. E*, **57**, 6761 (1998).

[4] M.R. Anderson, J.W. Baughn. *J. Heat Transfer*, **126**, 339 (2004).

[5] H. Zink, V.A. Belyakov. *JETP Lett.*, **63**, 43 (1996).

[6] H. Zink, V.A. Belyakov. *JETP*, **85**, 285 (1997).

[7] V.A. Belyakov, I.W. Stewart, M.A. Osipov. *JETP*, **99**, 1 (2004).

[8] V.A. Belyakov, I.W. Stewart, M.A. Osipov. *Phys. Rev. E*, **71**, 051708 (2005).

[9] V.A. Belyakov. *JETP Lett.*, **76**, 88 (2002).

[10] N.W. Roberts, J.-P.S. Guillou, H.F. Gleeson, I. Kirar, S.J. Watson, E.O. Arikainen. *Mol. Cryst. liq. Cryst.*, **411**, 57 (2004).

[11] N.W. Roberts, H.F. Gleeson, N. Bowring, A. Seed, J.W. Goodby, M. Hird. *J. mater. Chem.*, **13**, 353 (2003).

[12] S. Serak, A. Kovalev, A. Agashkov, H.F. Gleeson, S.J. Watson, V. Reshetnyak, O. Yaroshchuk. *Opt. Commun.*, **187**, 235 (2001).

[13] G.R. Fowles. *Introduction to Modern Optics*. Holt, Rinehart and Winston, New York (1975).

[14] F.A. Jenkins, H.E. White. *Foundation of Optics*. Mc Graw Hill (1987).

[15] F.Z. Yang, H.J. Gao, J.R. Sambles. *J. appl. Phys.*, **92**, 1744 (2002).

[16] A. Sugimura, G.R. Luckhurst, Z. Ou-Yang. *Phys. Rev. E.*, **52**, 681 (1995).

[17] A. Sugimura, K. Matsumoto, Z. Ou-Yang, M. Iwamoto. *Phys. Rev. E.*, **54**, 5217 (1996).